

## Article

# Novel High-Throughput Microwell Spectrophotometric Assay for One-Step Determination of Lorlatinib, a Novel Potent Drug for the Treatment of Anaplastic Lymphoma Kinase (ALK)-Positive Non-Small Cell Lung Cancer

Abdullah M. Al-Hossaini, Ibrahim A. Darwish \*  and Hany W. Darwish \*

Department of Pharmaceutical Chemistry, College of Pharmacy, King Saud University, P.O. Box 2457, Riyadh 11451, Saudi Arabia

\* Correspondence: idarwish@ksu.edu.sa (I.A.D.); hdarwish@ksu.edu.sa (H.W.D.)

**Abstract:** *Background and Objectives:* Lorlatinib (LOR) belongs to the third-generation anaplastic lymphoma kinase (ALK) tyrosine kinase inhibitors. People who are diagnosed with ALK-positive metastatic and advanced non-small cell lung cancer (NSCLC) are eligible to get it as a first-line treatment option after it was given the approval by “the Food and Drug Administration (FDA)”. However, no study has described constructing high-throughput analytical methodology for LOR quantitation in dosage form. For the first time, this work details the construction of a high-throughput, innovative microwell spectrophotometric assay (MW-SPA) for single-step assessment of LOR in its tablet form, for use in pharmaceutical quality control. *Materials and Methods:* Assay depended on charge transfer complex (CTC) formation between LOR, as electron donor, with 2,3-dichloro-3,5-dicyano-1,4-benzoquinone (DDQ), as  $\pi$ -electron acceptor. Reaction conditions were adjusted, the CTC was characterized by ultraviolet (UV)-visible spectrophotometry and computational molecular modeling, and its electronic constants were determined. Site of interaction on LOR molecule was allocated and reaction mechanism was suggested. Under refined optimum reaction conditions, the procedures of MW-SPA were performed in 96-well assay plates, and the responses were recorded by an absorbance plate reader. Validation of the current methodology was performed in accordance with guidelines of “the International Council on Harmonization (ICH)”, and all validation parameters were acceptable. *Results:* Limits of detection and quantitation of MW-SPA were 1.8 and 5.5  $\mu\text{g}/\text{well}$ , respectively. The assay was applied with great success for determining LOR in its tablets. *Conclusions:* This The assay is straightforward, economic and has high-throughput characteristics. Consequently, the assay is recommended as a valuable analytical approach in quality control laboratories for LOR’s tablets’ analysis.



**Citation:** Al-Hossaini, A.M.; Darwish, I.A.; Darwish, H.W. Novel High-Throughput Microwell Spectrophotometric Assay for One-Step Determination of Lorlatinib, a Novel Potent Drug for the Treatment of Anaplastic Lymphoma Kinase (ALK)-Positive Non-Small Cell Lung Cancer. *Medicina* **2023**, *59*, 756. <https://doi.org/10.3390/medicina59040756>

Academic Editors: Mohammed M. Alanazi and Konstantinos Dimas

Received: 2 February 2023

Revised: 6 April 2023

Accepted: 11 April 2023

Published: 13 April 2023

**Keywords:** 2,3-dichloro-3,5-dicyano-1,4-benzoquinone; lorlatinib; non-small cell lung cancer; charge transfer complex; spectrophotometry; high throughput

## 1. Introduction

Because it is primary main cause of death in both sexes all over world, cancer is a serious global health problem that has to be addressed. In the year 2020, it was anticipated that 18.1 million people would be diagnosed with cancer worldwide. When considering all forms of cancer, lung cancer is the one that occurs in the second most people around the world. It is most frequent kind of cancer to affect men and second most common form of cancer to affect women. In the year 2020, there were more than 2.2 million newly diagnosed cases of lung cancer which makes it the largest cause of cancer-related mortality [1] and is responsible for the most deaths. It is important to note that lung cancer is subdivided into small-cell and non-small-cell lung cancer (NSCLC). NSCLC is responsible for roughly 80–85 percent of the total cases of lung cancer. Main treatment options for NSCLC include



**Copyright:** © 2023 by the authors. Licensee MDPI, Basel, Switzerland. This article is an open access article distributed under the terms and conditions of the Creative Commons Attribution (CC BY) license (<https://creativecommons.org/licenses/by/4.0/>).

surgery, radiotherapy, and chemotherapy. For localized stage I and stage II of NSCLC, surgery and radiotherapy are usually useful; however, they are not authorized for advanced stages of NSCLC [2,3]. For ~80% of all patients with NSCLC, chemotherapy is usually recommended as a superior first-line treatment regime because it has been shown to increase both longevity and quality of life [4–6].

First-generation tyrosine kinase inhibitors such as gefitinib, erlotinib, and others have been widely prescribed [7,8]; however, a large proportion of patients have a chromosomal rearrangement that results in a fusion gene for anaplastic lymphoma kinase (ALK) and echinoderm microtubule-associated protein like 4 (EML4). The created gene causes constitutive activity of the kinase protein, and ultimately leads to increased cell carcinogenesis and induces malignant phenotype [9–11]. First generation tyrosine kinase inhibitors are unable to hinder fusion protein kinase activity. Therefore, drug discovery researchers were directed to discover novel drugs for treating patients with NSCLC including those harbor EML4/ALK proteins. The efforts of the researchers ultimately lead to the emerging of most potent third generation ALK inhibitor drugs, which gave a special interest and clinical benefits in treatment of ALK-positive patients NSCLC who are not responding to the earlier generations of ALK inhibitors.

Lorlatinib (LOR) is the first member of the third generation of ALK inhibitors [12,13]. Because of the clinical success of LOR, US-FDA on 3 March 2021, has been approved LOR for patients with metastatic NSCLC whose tumors are ALK-positive, distinguished by an FDA-approved test [14]. LOR was also approved by the European Medicines Agency (EMA) for treating patients with advanced and ALK-positive NSCLC [15]. LOR is sold in the markets under the trade name of Lorbena<sup>®</sup> tablets “Pfizer Inc., New York, NY, USA”. Recommended dose of LOR is 100 mg orally once daily [16].

The therapeutic benefits of LOR, in terms of its potency and safety, is principally depending on pharmaceutical formulation quality (Lorbena<sup>®</sup> tablets). Also, the therapeutic success of LOR is expected to be encouraging to the pharmaceutical companies for the development of new pharmaceutical preparations for LOR once the patent of Lorbena<sup>®</sup> tablets for Pfizer expires. Therefore, LOR determination in its pharmaceutical tablets would be necessary. To achieve this goal, a proper analytical method with high throughput is vital. Literature review revealed that only one analytical technology exists for determination of LOR; this technology is liquid chromatography [17–22]. Most of the existing chromatographic methods [18–22] relied on the expensive and instrumental intensive tandem mass spectrometric detectors and devoted to the analysis of LOR in biological samples. Only one chromatographic method is published for determining LOR in its bulk and pharmaceutical formulation [17]. The standards approach for quality control of pharmaceuticals require simple and high-throughput procedures, rather than the chromatographic procedures which usually have limited throughput. Because it allows the analysis of dozens, hundreds, or even thousands of samples every day in a given laboratory or on a specific instrument, high-throughput analysis is becoming increasingly significant in the pharmaceutical sector. This approach is important in the speedy identification of pharmaceutical entities, testing the uniformity of pharmaceutical formulations [23–25].

This manuscript designates, for the first time, development and validation of new microwell spectrophotometric assay (MW-SPA) with high-throughput for determination of LOR in pharmaceutical quality control laboratories. MW-SPA, described herein, is based on formation of colored charge-transfer complex (CTC) between LOR (electron donor), 2,3-dichloro-5,6-dicyano-1,4-benzoquinone (DDQ) ( $\pi$ -electron acceptor). Procedures of MW-SPA are performed in 96-well assay plates and absorbances are recorded by absorbance plate reader.

## 2. Experimental

### 2.1. Apparatus

A double-beam ultraviolet-visible spectrophotometer (V-530: JASCO Co., Ltd., Kyoto, Japan) was utilized for recording absorption spectra. Absorbance microplate reader

(ELx808: Bio-Tek Instruments Inc., Winooski, VT, USA) empowered by KC Junior software, provided with the instrument. The reader adapts a top-reading mode, and it is also equipped with a built-in heating system which enables the control of the temperature and maintain the temperature of the assay plates at the desired temperature. It can also apply a shaking action for 1 min for mixing the reagent with the analyte and settle a brief time (300 ms) after shaking before measuring the absorbances.

## 2.2. Chemicals and Materials

Lorlatinib (LOR) was purchased from “Selleck Chemicals (Houston, TX, USA)”. Purity was claimed to be 99.73% and solution stability was assured for a minimum of seven days on refrigeration. Lorbrena<sup>®</sup> tablets “Pfizer Inc., New York, NY, USA” were kindly donated by SFDA (Riyadh, Saudi Arabia) and its potency was claimed to be 100 mg of LOR per tablet. DDQ was purchased from “Sigma-Aldrich Chemicals Co. (St. Louis, MO, USA)”; its solution (0.4%, *w/v*, in methanol) was freshly prepared. Corning<sup>®</sup> 96-well transparent polystyrene assay plates with flat bottoms were purchased from Merck & Co., Inc. (Rahway, NJ, USA). Adjustable single and 8-channel pipettes (Finnpipette<sup>™</sup>) were obtained from Thermo Fisher Scientific Inc. (Waltham, MA, USA). Reagent reservoirs (BRAND<sup>®</sup> PP) with cover lids for dispensing the solutions by the 8-channel pipettes were purchased from “Merck KGaA (Darmstadt, Germany)”. Reagents and solvents were of spectroscopic grade “Fisher Scientific, California, CA, USA”.

## 2.3. Preparation of Standard LOR Solutions

LOR stock solution was prepared by dissolving 20 mg ( $8.13 \times 10^{-2}$  mole) of LOR in 10 mL methanol. This stock solution ( $4.9 \times 10^{-3}$  M) was diluted with methanol to acquire working solutions of LOR with concentrations suitable for the corresponding study.

## 2.4. Preparation of Tablets Sample Solution

Ten lorbrena<sup>®</sup> tablets were ground into a powdered form. In a 50-mL calibrated flask, a precise amount of the fine powder equal to 100 mg of LOR was transferred. Approximately 15 mL of methanol was added, and the mixture was vigorously shaken to dissolve LOR completely. The contents of the flask were filtered out, and the initial fraction of the filtrate was omitted. Filtrate was then diluted with methanol to yield 50–2000  $\mu\text{g mL}^{-1}$  LOR solutions. These solutions were analyzed for their nominated LOR concentrations by MW-SPA.

## 2.5. Association Constant and Molar Ratio Calculation

The association constant of LOR-DDQ CTC and its molar ratio were determined according to the methods described by Benesi-Hildebrand [26] and Job [27], respectively. For calculation of the association constant, a series of LOR solutions of varying concentrations ( $7.66 \times 10^{-5}$ – $9.23 \times 10^{-4}$  M) were equilibrated for  $\sim 5$  min at  $25 \pm 2$  °C with fixed concentration of DDQ ( $5.51 \times 10^{-3}$  M). Absorbances of the mixed equilibrated solutions were exploited for Benesi-Hildebrand plot generation. The results of regression analysis of the plot were used for computing the association constant.

For determination of LOR-DDQ ratio by “Job’s method” [27], equimolar solutions ( $4.9 \times 10^{-3}$  M) of LOR and DDQ reagent were used to make up different complementary reaction proportions (0:00, 25:175, 50:150, 100:100, 125:75, 150:50, 175:25, and 200:0). The measured absorbances were graphed versus  $[\text{LOR}]/[\text{LOR} + \text{DDQ}]$  and molar ratio of LOR/DDQ reaction was calculated using the generated plot.

## 2.6. Procedure of MW-SPA

Wells of 96-microwell assay plates were dispensed with aliquots (100  $\mu\text{L}$ ) of standard or tablet sample solution containing different concentrations of LOR (5–200 g). After addition of 100  $\mu\text{L}$  of a DDQ solution (0.4%, *w/v*), reaction was left to run for 5 min at  $25 \pm 2$  °C. Absorbance microplate reader was used to measure responses at 460 nm.

### 3. Results and Discussion

#### 3.1. Methodology and Strategy for Assay Development

Spectrophotometric assays are widely used in pharmaceutical industries [28–30]. These assays gained their importance and wide applications because they can be readily automated with spectrophotometric analyzers, that enable the analysis of hundreds of samples for the quality control assessment of pharmaceutical formulations, such as testing uniformity of contents and dissolution testing of tablets. The CT reactions have been widely employed as a basis for developing many spectrophotometric assays for the purpose of quality control of pharmaceuticals [31–34]. These assays are simple and rapid. Obviously, the chemical structure of LOR contains multiple electron-donating sites (e.g., amino group nitrogen atoms and ether-oxygen atom), which may contribute to the formation of CTC with electron acceptors. As revealed from an intensive literature review, CT reaction of LOR was not published yet. Therefore, our study is considered the first methodology in this area. DDQ is a versatile reagent which has been successfully utilized in varied chemical reactions and applications [35,36]. DDQ is commercially available, user-friendly, shelf-stable, solvent-soluble, and frequently produces non-toxic byproducts during its reactions. Alzoman et al. [37] established that DDQ is one of the most reactive acceptors in a prior work incorporating CT reactions with numerous polyhalo-/polycyanoquinone electron acceptors, and as a result, it has been widely used in the creation of several CT-based spectrophotometric tests for pharmaceuticals [37–40]. Due of these factors, DDQ was chosen as the electron acceptor for the MW-SPA presented here.

The conventional practice of the spectrophotometric assays, including CT reactions, usually employ volumetric flasks/cuvettes in the analysis, thus these assays have limited throughputs that do not meet the needs of quality control laboratories for the processing of pharmaceutical formulations [23–25]. In addition, the conventional CT-based assays consume large volumes of costly and more prominently it may cause analysts' toxicity [41–44]. As a result, developing new methodologies of higher throughput and utilizing small volumes of organic solvents was considered in constructing CT-based assays. Recently, our laboratory successfully employed absorbance microplate reader in adopting MW-SPA for quantitation of active constituents in their dosage forms [45]. These assays provided high throughput analysis and consumed low organic solvents volumes. For these reasons, the present study has undertaken the development of this methodology for LOR.

#### 3.2. Absorption Spectra and Band Gap Energy

An LOR solution UV-visible absorption spectra ( $4.92 \times 10^{-4}$  M, in methanol) was measured (Figure 1) and it displayed existence of two absorption maxima ( $\lambda_{\max}$ ) at 298 and 390 nm. When different concentrations of LOR solutions ( $0.77 \times 10^{-4}$ – $9.23 \times 10^{-4}$  M) were mixed with a fixed concentration of DDQ solution ( $5.51 \times 10^{-3}$  M), the reaction between LOR and DDQ was permitted to occur at  $25 \pm 2$  °C, and reaction mixture absorption spectra were measured vs. a DDQ reagent blank solution (Figure 1). Red color product with absorbance maximum of 460 nm was obtained and its intensity grew as the LOR concentration in reaction solution increased. This characteristic was clearly observed throughout the process of producing a new product from a reaction. The shape and pattern of resulting absorption band was comparable to DDQ radical anion as detailed in literature [37–40]. Hence, reaction was assumed to be a CT reaction involving LOR (electron donor, D) and DDQ ( $\pi$ -electron acceptor, A), and reaction continued in methanol (as an example of polar solvent) to create a CT complex (D-A), which was then dissociated by methanol giving radical anion of DDQ ( $A^{\bullet-}$ ), as shown in Figure 1A.

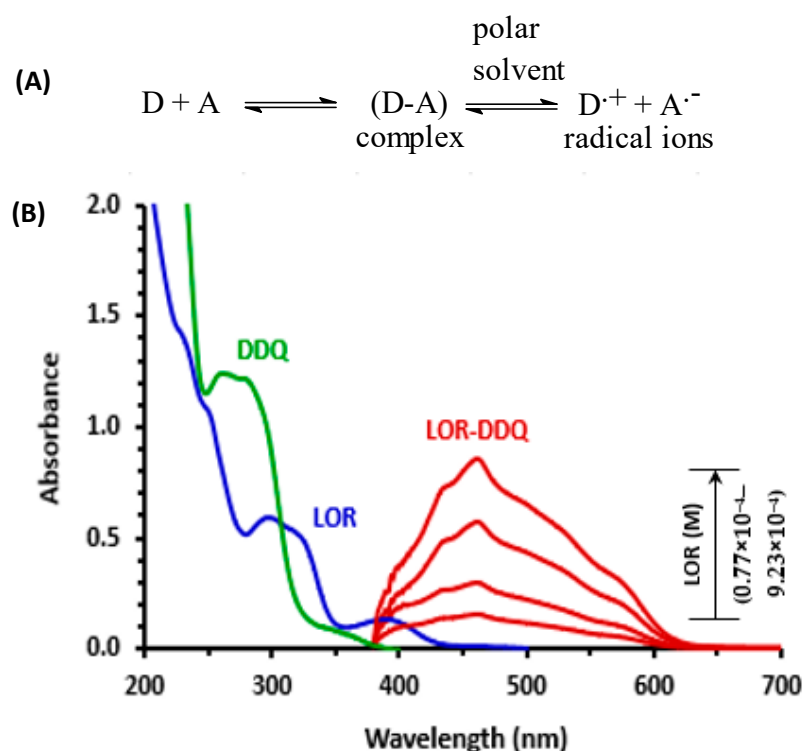


**Figure 1.** Panel (A): CT reaction between donor (D) and acceptor (A). Panel (B): Absorption spectra of lorlatinib, LOR ( $4.92 \times 10^{-4}$  M), 2,3-dichloro-3,5-dicyano-1,4-benzoquinone, DDQ ( $5.51 \times 10^{-3}$  M), and reaction mixtures (LOR-DDQ) containing varying concentrations of LOR ( $0.77 \times 10^{-4}$  M– $9.23 \times 10^{-4}$  M) and a fixed concentration of DDQ ( $5.51 \times 10^{-3}$  M); all solutions were in methanol.

Band gap energy ( $E_g$ ), defined as least amount of energy essential to excite an electron and cause its transition from low-energy valence band to the high-energy one and contribute to the formation of the formation of the CTC band, was determined according to procedures designated by Karipcin et al. [46].  $E_g$  value was 2.7036 eV. This small value indicated easiness of electron transfer from LOR to DDQ.

### 3.3. Reaction Conditions' Optimization

For determine utmost suitable solvent for optimal reaction, reaction between LOR and DDQ was performed in many solvents possessing different dielectric constants [47] and polarity indexes [48]. Results indicated that slight shifts in  $\lambda_{max}$  accompanied with changes in molar absorptivity ( $\epsilon$ ) occurred. Reaction in solvents possessing both high dielectric constants and polarity (methanol and acetonitrile) gave better  $\epsilon$  values than those in solvents with low dielectric constants and polarity (diethyl ether and dichloroethane) did. This effect was explained by the fact that the process of transferring electron from electron donor molecule (LOR) to electron acceptor (DDQ) is favored in polar solvents and diminished in non-polar solvents. In all subsequent steps, methanol was utilized as the proper solvent. At  $25 \pm 2$  °C the reaction in methanol was immediate. The effect of DDQ concentration was studied by performing reaction using varying concentrations of DDQ (0.1–1%,  $w/v$ ). Results revealed that color intensity of CTC increases as the DDQ concentration increases and the maximum color intensity was achieved when the DDQ concentration ranged from 0.25 to 0.5% ( $w/v$ ), beyond which the color intensity decreased (Figure 2). Accordingly, DDQ at a concentration of 0.4% ( $w/v$ ) was utilized in succeeding practical work. A summary of optimum reaction conditions was given in Table 1.

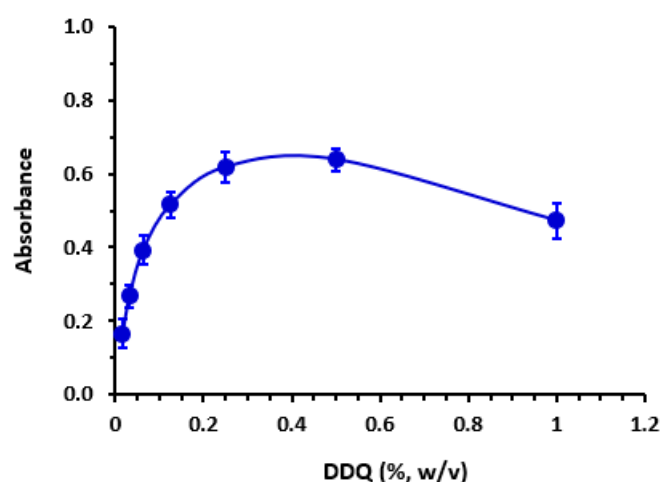


**Figure 2.** The effect of 2,3-dichloro-3,5-dicyano-1,4-benzoquinone (DDQ) concentration on charge transfer (CT) reaction with LOR ( $6.15 \times 10^{-4}$  M, in methanol).

**Table 1.** Optimization of MW-SPA experimental conditions.

Condition	Investigated Range	Optimal Value
DDQ conc. (% w/v)	0.1–1	0.4
Solvent	Different <sup>a</sup>	Methanol
Reaction time (min)	0–30	Instantaneous <sup>b</sup>
$\lambda_{\max}$ (nm)	350–750	460 <sup>c</sup>

<sup>a</sup> Solvents used were acetonitrile, methanol, ethanol, propanol, diethyl ether, dichloroethane, and chloroform.

<sup>b</sup> Measurements on plate reader were performed within 5 min. <sup>c</sup> Measurements on plate reader were performed at 450 nm.

### 3.4. Electronic Constants and Properties

The relevant electronic constants and properties of the LOR-DDQ CTC were determined according to the methods described in previous reports [26,49–53]. These constants and properties were the association constant [26], derived from Benesi-Hildebrand plot (Figure 3), standard free energy change [49], ionization potential [50], resonance energy [51], oscillator strength [52], and transition dipole moment [53]. Determination methods and obtained values were summarized in Table 2. Obviously, the big value of the association constant and low value of standard free energy change suggest that interaction between LOR and DDQ done simply and formed LOR-DDQ CTC was adequately stable. In addition, the high value of molar absorptivity of CTC enables the development of a sensitive assay for LOR.

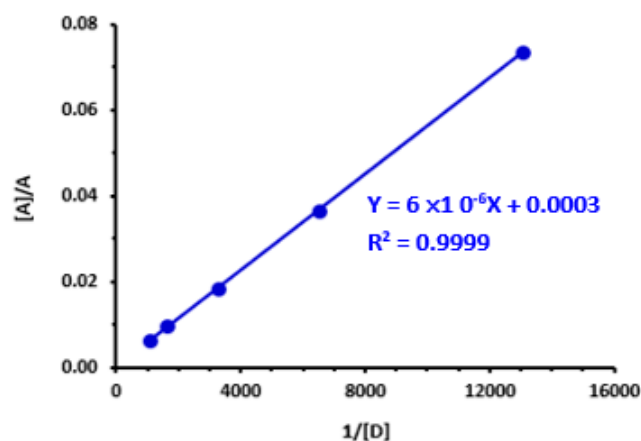


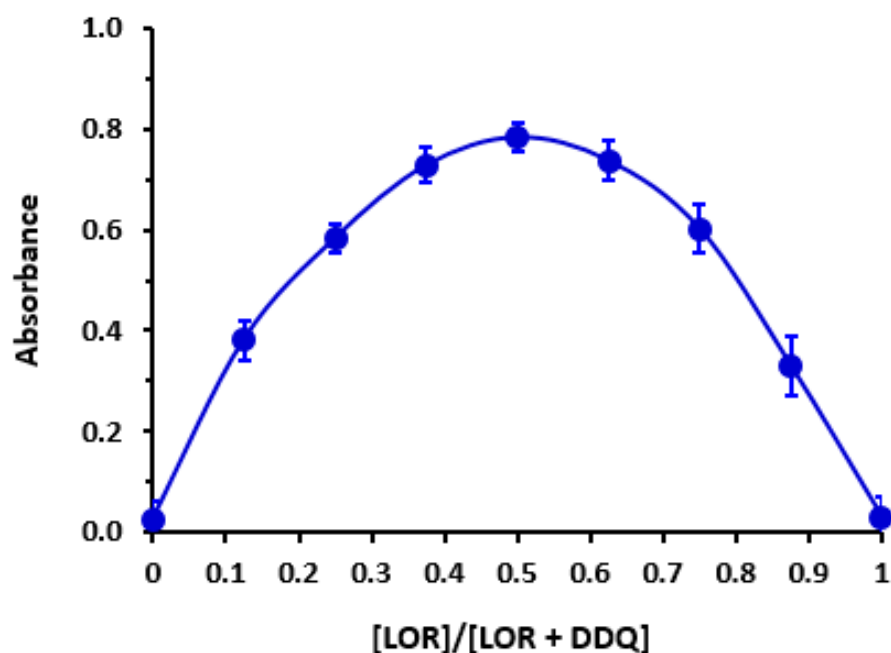
**Figure 3.** Benesi-Hildebrand plot for the formation of CTC of LOR with DDQ. Linear fitting equation and correlation coefficient ( $r^2$ ) are given on the plot. [A], A and [D] are molar concentrations of DDQ, absorbances of CTC, and molar concentration of LOR, respectively.

**Table 2.** Electronic constants/properties of CTC of LOR with DDQ.

Constant/Property	Method [Reference]	Equation/Procedure	Value
Molar absorptivity, $\epsilon$ ( $\text{L mol}^{-1} \text{ cm}^{-1}$ )	Benesi-Hildebrand [26]	Given in Section 2	$0.34 \times 10^3$
Association constant, $K$ ( $\text{L mol}^{-1}$ )	Benesi-Hildebrand [26]	The same equation used for calculating $\epsilon$	$0.52 \times 10^2$
Ionization potential, $I_p$ (eV)	Aloisi and Piganatro [50]	$I_p$ (eV) = $5.76 + 1.53 \times 10^{-4} \nu_{\text{CTC}}$	$1.06 \times 10^2$
Energy, $h\nu$ (eV)	Karipcin et al. [46]	From Tauc plot: $(\alpha h\nu)^2$ ( $\text{eV cm}^{-1}$ ) <sup>2</sup> Against Energy (eV)	2.7036
Resonance energy, $R_N$ (eV)	Briegleb and Czekalla [51]:	$R_N = 7.7 \times 10^{-4} / [(h \nu_{\text{CTC}} / R_N) - 3.5]$	0.7705
Transition dipole moment, $\mu$ (Debye)	Tsubumora and Lang [53]:	$\mu = 0.0958 [\epsilon_{\text{CTC}} \times \Delta\nu^{1/2} / \Delta\nu]^{1/2}$	$0.14 \times 10^2$
Oscillator strength, $f$	A.B.P. Lever [52]	$f = 4.32 \times 10^{-4} \int \epsilon_{\text{CTC}} d\nu^{1/2}$	0.4990
Standard free energy change, $\Delta G^0$ ( $\text{J mol}^{-1}$ )	Benesi-Hildebrand [26]	$\Delta G^0 = -2.303 RT \log K$	-9.811

### 3.5. Molar Ratio and Computational Charge Calculation

Using Job's continuous variation approach [27], molar ratio of LOR to DDQ was determined to be 1:1 (Figure 4), showing that only one site of LOR participated in creating CTC with DDQ. To identify this site among the several accessible electron-donating sites on LOR molecule (Figure 5), energy minimization was conducted on LOR molecule and electron density on each atom was determined. Energy minimization as well as charge calculation were carried out utilizing "CS Chem3D Ultra, version 16.0 (CambridgeSoft Corporation, Cambridge, MA, USA)" in conjunction with "molecular orbital computations software (MOPAC) and molecular dynamics computations software (MM2 and MMFF94)". Outcomes are shown in Table 3. Number 25 nitrogen atoms were assigned to have highest electron density (N25: aniline nitrogen). Taking into mind the molar ratio (1:1), it was hypothesized that the CT reaction between LOR and DDQ would proceed as seen in Figure 6.

**Figure 4.** Job's continuous variation plot for molar ratio determination of CT reaction of LOR with DDQ.

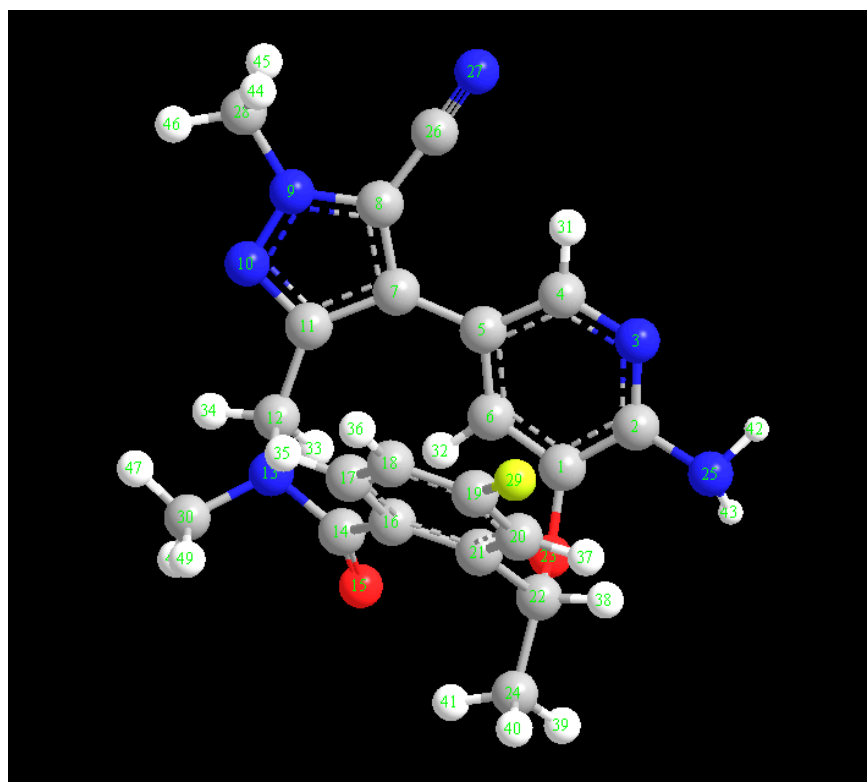


**Figure 5.** The energy minimized LOR molecule with atom numbers, and arrow points to atom with the highest electron density (N25) which participated in CTC formation between LOR and DDQ.

**Table 3.** Atom numbers, types, and their calculated charges on the energy minimized LOR molecule.

Atom Number	Atom Type	Charge	Atom Number	Atom Type	Charge
C(1)	Aromatic C, in benzene	0.0825	C(20)	Aromatic C, in benzene	−0.15
C(2)	Aromatic C, in benzene	0.41	C(21)	Aromatic C, in benzene	−0.1435
N(3)	Aromatic N, with s lone pair	−0.62	C(22)	Alkyl C, SP3	0.4235
C(4)	Aromatic C, in benzene	0.16	O(23)	Alcohol, ether O	−0.3625
C(5)	Aromatic C, in benzene	0	C(24)	Alkyl C, SP3	0
C(6)	Aromatic C, in benzene	−0.15	N(25)	Enamine, aniline N	−0.9
C(7)	Aromatic C, in 5-ring	0	C(26)	Cyano C	0.5371
C(8)	Aromatic C, in 5-ring	−0.1316	N(27)	Triple bond N	−0.5571
N(9)	Aromatic N, in 5-ring	0.314	C(28)	Alkyl carbon, SP3	0.2556
N(10)	Aromatic N, in 5-ring	−0.7068	F(29)	Fluorine	−0.19
C(11)	Aromatic C, in 5-ring	0.1078	C(30)	Alkyl carbon, SP3	0.3001
C(12)	Alkyl C, SP3	0.4811	H(31)–H(32)	H attached to C	0.15
N(13)	Amide N	−0.6602	H(33)–H(34)	H attached to C	0
C(14)	Amide carbonyl C	0.5438	H(35)–H(37)	H attached to C	0.15
O(15)	Carbonyl O, in amide	−0.57	H(38)–H(41)	H attached to C	0
C(16)	Aromatic C, in benzene	0.0862	H(42)–H(43)	H of enamine N	0.4
C(17)–C(18)	Aromatic C, in benzene	−0.15	H(44)–H(49)	H attached to C	0
C(19)	Aromatic C, in benzene	0.19			

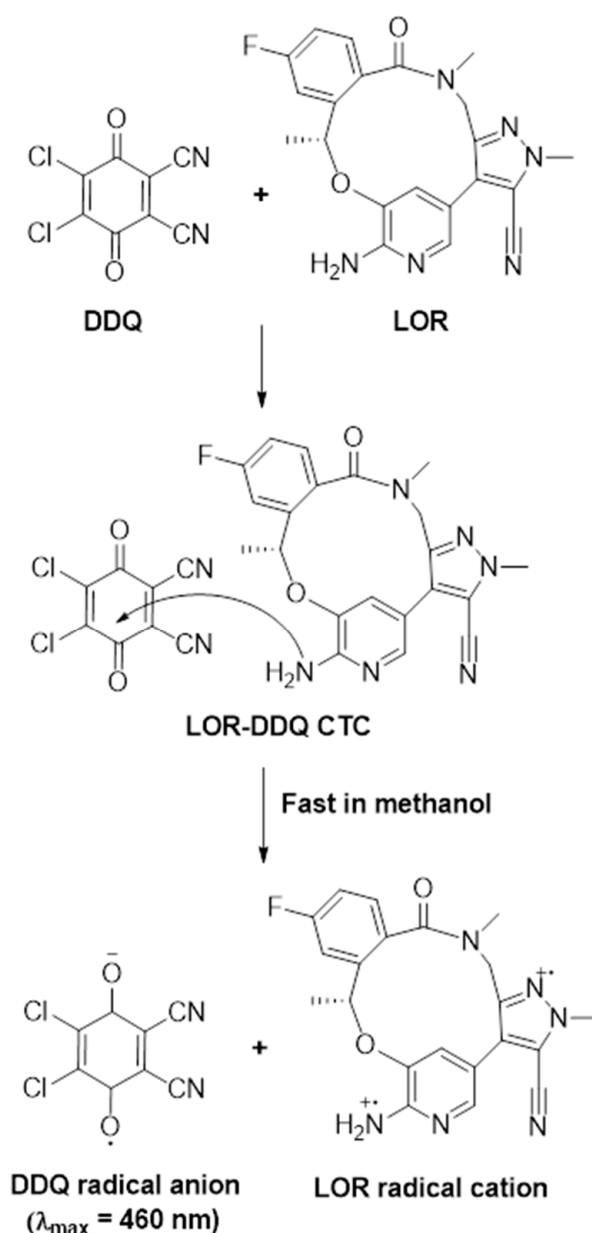


**Figure 6.** The scheme for the formation of the CTC between LOR and DDQ.

### 3.6. Development of MW-SPA

The optimum experimental conditions for carrying out reaction between LOR and DDQ in the 96-microwell assay plate were summarized in Table 1. The absorbances were measured by the absorbance microplate reader at 450 nm (nearest filter to  $\lambda_{\max}$  of CTC of LOR with DDQ, 460 nm).

### 3.7. Validation

#### 3.7.1. Linearity and Sensitivity

Under MW-SPA-optimized settings, calibration curve (Figure 7) was constructed, then linear regression analysis of the dataset was performed utilizing least-squares approach. Within the range of 5 to 200  $\mu\text{g}/\text{well}$  (100  $\mu\text{L}$ ), curve was linear, with 0.9996 correlation coefficient. Intercepts, slopes, and correlation coefficients (the three main components of linear fit) are displayed in Table 4. According to ICH criteria [54], LOD and LOQ were determined. LOD and LOQ values were 1.8 and 5.5  $\mu\text{g}/\text{well}$ , respectively. These limits are adequate for quantitation of LOR in only tablet's dosage form but not in biological

fluids. Table 4 provides a brief overview of proposed methodology's calibration and validation parameters.

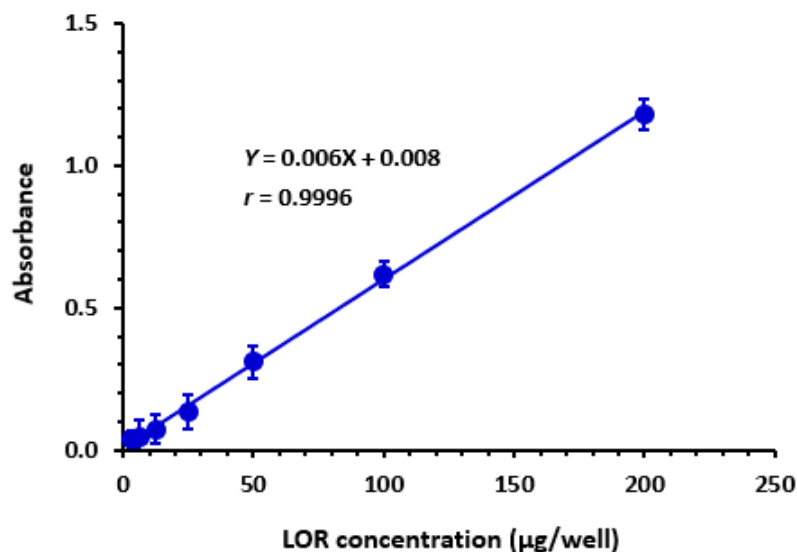


**Figure 7.** The calibration curve for the determination of LOR by MW-SPA via formation of CTC with DDQ. Linear regression equation and its correlation coefficient ( $r$ ) is given on calibration line.

**Table 4.** Calibration parameters for LOR quantitation by MW-SPA via formation of colored CTC with DDQ.

Parameter	Value
Linear dynamic range ( $\mu\text{g}/\text{well}$ )	5–200
Intercept (a)	0.008
Standard deviation of intercept ( $SD_a$ )	0.0033
Slope (b)	0.006
Standard deviation of slope ( $SD_b$ )	0.0004
Correlation coefficient ( $r$ )	0.9996
Limit of detection (LOD, $\mu\text{g}/\text{well}$ )	1.8
Limit of quantitation (LOQ, $\mu\text{g}/\text{well}$ )	5.5

### 3.7.2. Precision and Accuracy

Samples of LOR solutions with varied concentrations were utilized to ensure precisions of the proposed MW-SPA (Table 5). For intra- and inter-assay precision, RSD ranged from 0.15 to 1.76 and 1.12 to 1.86%, respectively. It was clear from small RSD values that the assay was highly precise. At the same levels of LOR concentrations as the precision experiments, assay's accuracy was assessed by recovery studies. According to Table 5, recovery values ranged from 98.1 to 103.1%, demonstrating high accuracy of current assay.

**Table 5.** MW-SPA precision at various LOR concentration levels.

Taken Concentration ( $\mu\text{g}/\text{well}$ )	Precision: Relative Standard Deviation (%)		Accuracy: Recovery (% $\pm$ SD) <sup>a</sup>
	Intra-Assay, $n = 3$	Inter-Assay, $n = 6$	
6.25	0.93	1.56	101.2 $\pm$ 0.84
12.5	0.15	1.25	99.6 $\pm$ 1.25
25	0.53	1.44	98.8 $\pm$ 1.51
50	0.86	1.12	100.5 $\pm$ 0.89
100	0.56	1.80	103.1 $\pm$ 2.12
200	1.76	1.86	101.4 $\pm$ 1.58

<sup>a</sup> Values are mean of three determinations.

### 3.7.3. Specificity and Interference

Specificity of proposed MW-SPA for LOR quantitation in tablets without any potential interference from the inactive excipients which are co-formulated with LOR is documented because of two main reasons. The first one is the measurements of LOR in the visible region (460 nm) which is far away from the UV-absorbing excipients which might be extracted from the tablets during the preparation of tablets solution. The second reason is the use of methanol for preparation of tablet solution which dissolve only LOR leaving the excipients because they do not dissolve in methanol.

### 3.7.4. Robustness and Ruggedness

MW-SPA robustness (impact of minor variation in assay variables on performance) was assessed. Concentration of DDQ, reaction time, and temperature were all altered by a factor of 10% from their optimum values (Table 1). Minor procedure variables didn't disturb assay results revealing assay suitability for routine LOR analysis.

Two analysts performed the experiment on three different days to test ruggedness. Since the maximum RSD  $\leq 2\%$ , the results derived from differences in analysis from one analyst to another and from day to day were determined to be reproducible.

### 3.8. Analysis of Lorbreña<sup>®</sup> Tablets

Successful validation results obtained depicted the appropriateness of current MW-SPA methodology for routine QC analysis of LOR-containing commercial pharmaceutical tablets. MW-SPA methodology was applied for assessing LOR in lorbreña<sup>®</sup> tablets. Computed mean value of labelled amount was  $101.3 \pm 1.64\%$  (Table 6).

**Table 6.** Analysis of lorbreña<sup>®</sup> tablets by the proposed MW-SPA.

Nominal Concentration ( $\mu\text{g/mL}$ )	Found Concentration <sup>a</sup> ( $\mu\text{g/mL}$ )	Recovery <sup>a</sup> (%)
62.5	63.22	$101.2 \pm 2.1$
500	507.18	$101.4 \pm 1.4$
1000	1032.03	$103.2 \pm 1.1$
2000	1993.56	$99.2 \pm 1.5$
	Mean	101.3
	SD	1.64

<sup>a</sup> Values are mean of three determinations.

## 4. Conclusions

UV-visible spectrophotometric analysis confirmed production of CTC between LOR and DDQ, as demonstrated by the emergence of a new absorption peak with maximal absorption peak at 460 nm. It was determined that molar ratio of CTC (LOR:DDQ) was 1:1. Molar absorptivity of CTC was dependent on both solvent's polarity index and dielectric constant. Reaction mechanism was hypothesized. The reaction between LOR and DDQ served as the basis for the development of a unique MW-SPA for analyzing LOR in bulk and tablets. Assay offers a high throughput, permitting a large number of samples to be analyzed in a short amount of time. Additionally, when employed in quality control laboratories, the assay is eco-friendly because it employs a very small volume of organic solvent.

**Author Contributions:** A.M.A.-H.: Investigation, Visualization, Data curation, Writing—review & editing. I.A.D.: Conceptualization, Methodology, Resources, Supervision, Writing—review & editing. H.W.D.: Investigation, Visualization, Data curation, Writing—review & editing. All authors have read and agreed to the published version of the manuscript.

**Funding:** This research was funded by the Researchers Supporting Project number (RSPD2023R812), King Saud University, Riyadh, Saudi Arabia.

**Data Availability Statement:** All data are available from the corresponding author.

**Acknowledgments:** The authors extend their appreciation to the Researchers Supporting Project number (RSPD2023R812), King Saud University, Riyadh, Saudi Arabia.

**Conflicts of Interest:** Authors declare no conflict of interest.

## References

1. Siegel, R.L.; Miller, K.D.; Fuchs, H.E.; Jemal, A. Cancer statistics. *CA Cancer J. Clin.* **2022**, *72*, 7–33. [CrossRef]
2. Rowell, N.P.; Williams, C.J. Radical radiotherapy for stage I/II non-small cell lung cancer in patients not sufficiently fit for or declining surgery (medically inoperable): A systematic review. *Thorax* **2001**, *56*, 628–638. [CrossRef] [PubMed]
3. Stand, T.E.; Brunsvig, P.F.; Johannessen, D.C.; Sundstrøm, S.; Wang, M.; Hornslien, K.; Bremnes, R.M.; Stensvold, A.; Garpestad, O.; Norstein, J. Potentially curative radiotherapy for non-small cell lung cancer in Norway: A population-based study of survival. *Int. J. Radiat. Oncol. Biol. Phys.* **2011**, *80*, 133–141. [CrossRef]
4. Tan, W.; Harris, J.E.; Huq, S. Non-Small Cell Lung Cancer. Available online: <http://emedicine.medscape.com/article/279960-overview> (accessed on 29 January 2023).
5. NSCLC Meta-Analyses Collaborative Group. Chemotherapy in addition to supportive care improves survival in advanced non-small-cell lung cancer: A systematic review and meta-analysis of individual patient data from 16 randomized controlled trials. *J. Clin. Oncol.* **2008**, *26*, 4617–4625. [CrossRef]
6. Non-Small Cell Lung Cancer Collaborative Group. Chemotherapy and supportive care versus supportive care alone for advanced non-small cell lung cancer. *Cochrane Database Syst. Rev.* **2010**, *5*, CD007309. [CrossRef]
7. Cohen, M.H.; Williams, G.A.; Sridhara, R.; McGuinn, W.D., Jr.; Morse, D.; Abraham, S.; Rahman, A.; Liang, C.; Lostritto, R.; Baird, A.; et al. United States Food and Drug Administration drug approval summary: Gefitinib (ZD1839; Iressa) tablets. *Clin. Cancer Res.* **2004**, *10*, 1212–1218. [CrossRef]
8. Johnson, J.R.; Cohen, M.; Sridhara, R.; Chen, Y.F.; Williams, G.M.; Duan, J.; Gobburu, J.; Booth, B.; Benson, K.; Leighton, J.; et al. Approval summary for erlotinib for treatment of patients with locally advanced or metastatic non-small cell lung cancer after failure of at least one prior chemotherapy regimen. *Clin. Cancer Res.* **2005**, *11*, 6414–6421. [CrossRef]
9. Paulus, V.; Pana-Katatali, H.; Perol, M.; Paget-Bailly, S.; Trinquart, L.; Perol, D.; Calais, F.; Bonnetain, F.; Westeel, V. Maintenance therapy for advanced non-small cell lung cancer (NSCLC). *Cochrane Database Syst. Rev.* **2019**, *2019*, CD011631. [CrossRef]
10. Winslow, R.; Loftus, P. Advances Come in War on Cancer. WSJ. Available online: <https://www.wsj.com/articles/SB10001424052748704002104575291103764336126> (accessed on 12 April 2023).
11. Pfizer. Pfizer Oncology to Present New Clinical Data from Ten Molecules across Multiple Tumor Types. Available online: [https://www.pfizer.com/news/press-release/press-release-detail/pfizer\\_oncology\\_to\\_present\\_new\\_clinical\\_data\\_from\\_ten\\_molecules\\_across\\_multiple\\_tumor\\_types](https://www.pfizer.com/news/press-release/press-release-detail/pfizer_oncology_to_present_new_clinical_data_from_ten_molecules_across_multiple_tumor_types) (accessed on 29 January 2023).
12. Basit, S.; Ashraf, Z.; Lee, K.; Latif, M. First macrocyclic 3rd-generation ALK inhibitor for treatment of ALK/ROS1 cancer: Clinical and designing strategy update of lorlatinib. *Eur. J. Med. Chem.* **2017**, *134*, 348–356. [CrossRef]
13. Awad, M.M.; Shaw, A.T. ALK inhibitors in non-small cell lung cancer: Crizotinib and beyond. *Clin. Adv. Hematol. Oncol.* **2014**, *12*, 429–439.
14. U.S. Food & Drug Administration. FDA Approves Lorlatinib for Metastatic ALK-Positive NSCLC. Available online: <https://www.fda.gov/drugs/resources-information-approved-drugs/fda-approves-lorlatinib-metastatic-alk-positive-nsclc> (accessed on 29 January 2023).
15. European Medicines Agency. Lorviqua: Lorlatinib. Available online: <https://www.ema.europa.eu/en/medicines/human/EPAR/lorviqua> (accessed on 29 January 2023).
16. lorbrena® (Lorlatinib) Tablets, for Oral Use. Available online: [https://www.accessdata.fda.gov/drugsatfda\\_docs/label/2021/210868s004lbl.pdf](https://www.accessdata.fda.gov/drugsatfda_docs/label/2021/210868s004lbl.pdf) (accessed on 29 January 2023).
17. Anuradha, N.D.; Nizam, S.A. RP-HPLC method development and validation for the determination of lorlatinib in bulk and its pharmaceutical formulation. *World J. Pharm. Pharm. Sci.* **2023**, *8*, 114–21150.
18. De Leeuw, S.P.; de Bruijn, P.; Koolen, S.L.W.; Dingemans, A.-M.C.; Mathijssen, R.H.J.; Veerman, G.D.M. Quantitation of osimertinib, alectinib and lorlatinib in human cerebrospinal fluid by UPLC-MS/MS. *J. Pharm. Biomed. Anal.* **2023**, *225*, 115233. [CrossRef]
19. Chen, W.; Shi, Y.; Qi, S.; Zhou, H.; Li, C.; Jin, D.; Li, G. Pharmacokinetic study and tissue distribution of lorlatinib in mouse serum and tissue samples by liquid chromatography-mass spectrometry. *J. Anal. Methods Chem.* **2019**, *2019*, 7574369. [CrossRef]
20. Sparidans, R.W.; Li, W.; Schinkel, A.H.; Schellens, J.H.M.; Beijnen, J.H. Bioanalytical liquid chromatography-tandem mass spectrometric assay for the quantification of the ALK inhibitors alectinib, brigatinib and lorlatinib in plasma and mouse tissue homogenates. *J. Pharm. Biomed. Anal.* **2018**, *161*, 136–143. [CrossRef]
21. Gulikers, J.L.; van Veelen, A.J.; Sinkiewicz, E.M.J.; de Beer, Y.M.; Slikkerveer, M.; Stolk, L.M.L.; Tjan-Heijnen, V.C.G.; Hendriks, L.E.L.; Croes, S.; van Geel, R.M.J.M. Development and validation of an HPLC-MS/MS method to simultaneously quantify brigatinib, lorlatinib, pralsetinib and selpercatinib in human K2-EDTA plasma. *Biomed. Chromatogr.* **2023**, 5628. [CrossRef] [PubMed]

22. Li, W.; Perpinioti, N.; Schinkel, A.H.; Beijnen, J.H.; Sparidans, R.W. Bioanalytical assay for the new-generation ROS1/TRK/ALK inhibitor repotrectinib in mouse plasma and tissue homogenate using liquid chromatography-tandem mass spectrometry. *J. Chromatogr.* **2020**, *1144*, 122098. [CrossRef]
23. Wang, P.G. (Ed.) *High-Throughput Analysis in the Pharmaceutical Industry*, 1st ed.; CRC Press: Boca Raton, FL, USA, 2019.
24. Mennen, S.M.; Alhambra, C.; Allen, C.L.; Barberis, M.; Berritt, S.; Brandt, T.A.; Campbell, A.D.; Castañón, J.; Cherney, A.H.; Christensen, M.; et al. The evolution of high-throughput experimentation in pharmaceutical development and perspectives on the future. *Org. Process Res. Dev.* **2019**, *23*, 1213–1242. [CrossRef]
25. Welch, C.J. High throughput analysis enables high throughput experimentation in pharmaceutical process research. *React. Chem. Eng.* **2019**, *4*, 1895–1911. [CrossRef]
26. Benesi, H.A.; Hildebrand, J. *Physical Pharmacy*, 4th ed.; Lea & Febiger: Philadelphia, PA, USA, 1993; p. 266.
27. Job, P. Formation and stability of inorganic complexes in solution. *Ann. Chem.* **1928**, *9*, 113–203.
28. Görög, S. *Ultraviolet-Visible Spectrophotometry in Pharmaceutical Analysis*; CRC Press: New York, NY, USA, 2018.
29. Ahmed, S.; Rasul, A.; Masood, Z. *Spectrophotometry in Pharmaceutical Analysis*; LAP Lambert Academic Publishing: London, UK, 2011.
30. Gore, M.G. (Ed.) *Spectrophotometry and Spectrofluorimetry: A Practical Approach*, 2nd ed.; Oxford University Press: Oxford, UK, 2000.
31. Darwish, I.A. Analytical study for the charge transfer complexes of losartan potassium. *Anal. Chim. Acta* **2005**, *549*, 212–220. [CrossRef]
32. Darwish, I.A.; Refaat, I.H. Spectrophotometric analysis of selective serotonin reuptake inhibitors based on formation of charge-transfer complexes with tetracyanoquinodimethane and chloranilic acid. *J. AOAC Int.* **2006**, *89*, 326–333. [CrossRef] [PubMed]
33. El-Bagary, R.I.; Elkady, E.F.; Ayoub, B.M. Spectrophotometric methods based on charge transfer complexation reactions for the determination of saxagliptin in bulk and pharmaceutical preparation. *Int. J. Biomed. Sci.* **2012**, *8*, 204–208. [PubMed]
34. Kalyanaramu, B.; Rupakumari, G.; Ramarao, K.; Raghobabu, K. Development of new visible spectrophotometric methods for quantitative determination of sumatriptan succinate based on charge-transfer complex formation. *Int. J. Pharm. Pharm. Sci. Res.* **2011**, *1*, 47–51.
35. Alsharif, M.A.; Raja, Q.A.; Majeed, N.A.; Jassas, R.S.; Alsimaree, A.A.; Sadiq, A.; Naeem, N.; Mughal, E.U.; Alsantali, R.I.; Moussa, Z.; et al. DDQ as a versatile and easily recyclable oxidant: A systematic review. *RSC Adv.* **2021**, *11*, 29826–29858. [CrossRef] [PubMed]
36. Natarajan, P.; König, B. Excited-state 2,3-dichloro-5,6-dicyano-1,4-benzoquinone (DDQ\*) initiated organic synthetic transformations under visible-light irradiation. *Eur. J. Org. Chem.* **2021**, *2021*, 2145–2161. [CrossRef]
37. Alzoman, N.Z.; Sultan, M.A.; Maher, H.M.; Alshehri, M.M.; Wani, T.A.; Darwish, I.A. Analytical study for the charge-transfer complexes of rosuvastatin calcium with  $\pi$ -acceptors. *Molecules* **2013**, *18*, 7711–7725. [CrossRef]
38. Darwish, I.A.; Khalil, N.Y.; Alsaif, N.A.; Herqash, R.N.; Sayed, A.Y.A.; Abdel-Rahman, H.M. Charge-Transfer complex of linifanib with 2,3-dichloro-3,5-dicyano-1,4-benzoquinone: Synthesis, spectroscopic characterization, computational molecular modelling and application in the development of novel 96-microwell spectrophotometric assay. *Drug Des. Devel. Ther.* **2021**, *15*, 1167–1180. [CrossRef] [PubMed]
39. Khalil, N.Y.; Wani, T.A.; Darwish, I.A.; Assiri, I.S. Charge-transfer reaction of cediranib with 2,3-dichloro-3,5-dicyano-1,4-benzoquinone: Spectrophotometric investigation and use in development of microwell assay for cediranib. *Trop. J. Pharm. Res.* **2015**, *14*, 1667–1672. [CrossRef]
40. Raza, A.; Ansari, T.M. Application of 2,3-dichloro-5,6-dicyano-p-benzoquinone (DDQ) for spectrophotometric determination of caroverine in pharmaceutical formulations. *SOJ Pharm. Pharm. Sci.* **2017**, *4*, 1–4. [CrossRef]
41. Wennborg, H.; Bonde, J.P.; Stenbeck, M.; Olsen, J. Adverse reproduction outcomes among employees working in biomedical research laboratories. *Scand. J. Work Environ. Health* **2005**, *28*, 5–11. [CrossRef] [PubMed]
42. Lindbohm, M.L.; Taskinen, H.; Sallman, M.; Hemminki, K. Spontaneous abortions among women exposed to organic solvents. *Am. J. Indust. Med.* **1990**, *17*, 449–463. [CrossRef] [PubMed]
43. Wennborg, H.; Bodin, L.; Vainio, H.; Axelsson, G. Pregnancy outcome of personnel in Swedish biomedical research laboratories. *J. Occup. Environ. Med.* **2000**, *42*, 438–446. [CrossRef] [PubMed]
44. Kristensen, P.; Hilt, B.; Svendsen, K.; Grimsrud, T.K. Incidence of lymphohaematopoietic cancer at a university laboratory: A cluster investigation. *Eur. J. Epidemiol.* **2008**, *23*, 11–15. [CrossRef] [PubMed]
45. Khalil, N.Y.; Al Qhatani, M.N.; Al Qubaisi, K.A.; Sayed, A.Y.; Darwish, I.A. Development of two innovative 96-microwell-based spectrophotometric assays with high throughput for determination of fluoroquinolone antibiotics in their pharmaceutical formulations. *J. Appl. Spectrosc.* **2022**, *89*, 1–9. [CrossRef]
46. Makuła, P.; Pacia, M.; Macyk, W. How to correctly determine the band gap energy of modified semiconductor photocatalysts based on UV-Vis spectra. *J. Phys. Chem. Lett.* **2018**, *9*, 6814–6817. [CrossRef]
47. Vogel, A.I.; Tatchell, A.R.; Furnis, B.S.; Hannaford, A.J.; Smith, P.G. *Vogel's Textbook of Practical Organic Chemistry*, 5th ed.; Longman Group UK Ltd.: England, UK, 1989.
48. Polarity Index. Available online: <http://macro.lsu.edu/howto/solvents/polarity%20index.htm> (accessed on 29 January 2023).
49. Pandeeswaran, M.; Elango, K. Solvent effect on the charge transfer complex of oxatomide with 2, 3-dichloro-5, 6-dicyanobenzoquinone. *Spectrochim. Acta* **2006**, *65*, 1148–1153. [CrossRef]
50. Aloisi, G.; Pignataro, S. Molecular complexes of substituted thiophens with  $\sigma$  and  $\pi$  acceptors. Charge transfer spectra and ionization potentials of the donors. *J. Chem. Soc. Faraday Trans.* **1972**, *69*, 534–539. [CrossRef]

51. Briegleb, G.; Czekalla, J. Intensity of electron transition bands in electron donator–acceptor complexes. *Z. Physik. Chem.* **1960**, *24*, 37. [[CrossRef](#)]
52. Lever, A.B.P. *Inorganic Electronic Spectroscopy*, 2nd ed.; Elsevier: Amsterdam, The Netherlands, 1985; p. 161.
53. Tsubumora, H.; Lang, R. Molecular complexes and their spectra. XIII. complexes of iodine with amides, diethyl sulfide and diethyl disulfide. *J. Am. Chem. Soc.* **1961**, *83*, 2085–2092. [[CrossRef](#)]
54. ICH. *International Council for Harmonisation of Technical Requirements for Pharmaceuticals for Human Use*; ICH Harmonised Guideline, Validation of Analytical Procedure: Q2(R2); ICH: Geneva, Switzerland, 2022.

**Disclaimer/Publisher’s Note:** The statements, opinions and data contained in all publications are solely those of the individual author(s) and contributor(s) and not of MDPI and/or the editor(s). MDPI and/or the editor(s) disclaim responsibility for any injury to people or property resulting from any ideas, methods, instructions or products referred to in the content.